Cationic Ascorbate Peroxidase Isoenzyme II from Tea: Structural Insights into the Heme Pocket of a Unique Hybrid Peroxidase†

Hendrik A. Heering,‡ Marcel A. K. Jansen,§ Roger N. F. Thorneley,§ and Giulietta Smulevich*,‡

Dipartimento di Chimica, Università di Firenze, Via G. Capponi 9, I-50121 Firenze, Italy, and Department of Biological Chemistry, John Innes Centre, Norwich NR4 7UH, United Kingdom

Received March 26, 2001; Revised Manuscript Received June 18, 2001

ABSTRACT: The novel class III ascorbate peroxidase isoenzyme II from tea leaves (TcAPXII), with an unusually high specific ascorbate peroxidase activity associated with stress response, has been characterized by resonance Raman (RR), electronic absorption, and Fourier transform infrared (FT-IR) spectroscopies. Ferric and ferrous forms and the complexes with fluoride, cyanide, and CO have been studied at various pH values. The overall blue shift of the electronic absorption spectrum, the high RR frequencies of the core size marker bands, similar to those of 6-coordinate low-spin heme, and the complex RR spectrum in the low-frequency region of ferric TcAPXII indicate that this protein contains an unusual 5-coordinate quantum mechanically mixed-spin heme. The spectra of both the fluoride and the CO adducts suggest that these exogenous ligands are strongly hydrogen-bonded with a residue that appears to be unique to this peroxidase. Electronic absorption spectra also emphasize structural differences between the benzhydroxamic acid binding sites of TcAPXII and horseradish peroxidases (HRPC). It is concluded that TcAPXII is a paradigm peroxidase since it is the first example of a hybrid enzyme that combines spectroscopic signatures, structural elements, and substrate specificities previously reported only for distinct class I and class III peroxidases.

Peroxidases are ubiquitous heme proteins that catalyze the oxidation of a range of substrates by hydrogen peroxide and/or organic hydroperoxides. On the basis of sequence homologies, the peroxidases of higher plants are currently classified as either ascorbate (EC 1.11.1.11) or classical (EC 1.11.1.7) peroxidases (*1*). Ascorbate (members of class I) peroxidases use ascorbate as a reducing substrate and play an important role in scavenging reactive oxygen species (*2*). Thus, ascorbate peroxidase isozymes have been implicated in tolerance to a range of abiotic stress conditions (*3*). These enzymes are found in all higher plants. They are localized in the chloroplast and cytosol [see ref *4* and referenced cited therein] where they often accumulate in response to stress conditions (*5*). Classical (also known as class III) peroxidases are secreted to the apoplast, hence they are also known as secretory peroxidases. These enzymes oxidize phenolic compounds at high rates and have been implicated in a range of physiological processes such as the cross-linking of phenolic compounds to proteins and polysaccharides and/or the deposition of polyphenols and lignin in the cell wall (*6*), suberization (*7*), pathogen resistance (*8*), UV-B tolerance (*9*), and the oxidative degradation of the major endogenous auxin, indole-3-acetic acid (*10*−*12*).

Notwithstanding the functional differences between ascorbate and classical peroxidases, several structural elements and amino acid residues are conserved, particularly in the vicinity of the heme group. The conserved catalytic distal His42 and Arg38 residues [horseradish peroxidase, isoenzyme C (HRPC)[1] numbering, see ref *13*] that are localized on the distal side of the heme, play a concerted role in H_2O_2 binding to the ferric resting state and subsequent $2e^-$ oxidation of the enzyme to compound I [reviewed in ref *14*]. A conserved aromatic residue (typically a Trp in class I peroxidases and a Phe in classes II and III), located next to the distal His42, is thought to modulate the kinetic properties and substrate specificity of the enzyme (*13*). Conserved residues on the proximal side of the heme include Val164, His170, and Asp247 (HRPC numbering). Classification of peroxidases involves the recognition of helical segments in the structure. These helical structures are preserved within each family, although the connecting loops may vary in length. Thus, ascorbate peroxidases possess an additional

† This work was supported by grants from the Italian Consiglio Nazionale delle Ricerche (CNR) and Ministero della Ricerca Scientifica e dell'Universitá (MURST) to G.S. and from the European Union Training and Mobility of Researchers Program "Peroxidases in Agriculture, the Environment and Industry" (Contract ERB-FMRX-CT98-0200) to G.S. and R.N.F.T. H.A.H. and M.A.K.J. are funded by fellowships from the EU as part of the above program.

* To whom correspondence should be addressed: Tel +39 0552757596; fax +39 055 2476961; e-mail smulev@chim.unifi.it.

‡ Università di Firenze.

§ John Innes Centre.

[1] Abbreviations: APX, ascorbate peroxidase; BP 1, barley grain peroxidase; CCP, cytochrome *c* peroxidase; CIP, *Coprinus cinereus* peroxidase, expressed in *Aspergillus oryzae* (identical to ARP, *Arthromyces ramosus* peroxidase); HRPA2, horseradish peroxidase isoenzyme A2; HRPC, horseradish peroxidase isoenzyme C; metMb, metmyoglobin; NiOEP, nickel octaethylporphyrin; SBP, soybean peroxidase; TcAPXI and TcAPXII, tea cationic ascorbate peroxidase isoenzymes I and II, respectively; CT1, long-wavelength (>600 nm) porphyrin-to-metal charge transfer band; FT-IR, Fourier transform infrared; RR, resonance Raman; 5c, five-coordinate; 6c, six-coordinate; HS, high-spin; QS, quantum mechanically mixed-spin; LS, low-spin; BHA, benzhydroxamic acid; Tris, tris[hydroxymethyl]aminomethane.

10.1021/bi0106033 CCC: $20.00 © 2001 American Chemical Society
Published on Web 08/02/2001

short helix (B′) that is not present in classical peroxidases. Classical peroxidases possess three additional short helices (D′, F′, and F″) that are not present in ascorbate peroxidases (*13*). Further differences are the presence of cysteine bridges, calcium binding sites, glycosylation sites, and signal peptides for secretion in classical but not ascorbate peroxidases (*13*). The structural differences between ascorbate and classical peroxidases are reflected in their respective substrate affinities and kinetic properties. Thus, classical peroxidases have a relatively low specificity for ascorbate, while ascorbate peroxidases have a relatively low affinity for phenolic substrates. Classical plant peroxidases form a relatively stable compound I, compared to that of ascorbate peroxidases (*15, 16*).

Since ascorbate and classical peroxidases play very different physiological roles in planta, it is important to identify the structural determinants of their substrate affinity and reactivity. The recent purification and characterization of two classical peroxidases from tea, TcAPXI (*17*) and TcAPXII (*18*), which exhibited a high very specific activity for ascorbate, provides a unique opportunity to investigate these structure /function relationships. TcAPXII has the highest specific APX activity ever reported but a very low activity toward phenolic substrates. The amino acid sequences show that the two isoenzymes are distinct, but comparison with other peroxidases shows high homology with class III peroxidases and little similarity with pea cytosolic APX (*18*). Most notably, a Phe residue replaces the distal cavity Trp residue of pea APX and CCP. Furthermore, the TcAPXII sequence suggests the presence of cysteine bridges and Ca^{2+} binding sites not present in pea APX. The N-terminal sequence of TcAPXII suggests that it is monomeric, whereas pea APX is a dimer (*19*). These findings therefore indicate that structurally these two cationic isozymes from tea leaves belong to the family of classical peroxidases (class III).

These unusual "ascorbate-oxidizing class III peroxidases" may well constitute an evolutionary adaption that has coevolved with the high levels of polyphenols present in tea leaves. An intriguing question is which factors determine the high ascorbate oxidizing activity of TcAPXII. The current classification of peroxidases is based on the recognition of structural elements (*1*). However, relationships between specific structural elements and function have only been established in a few cases (*13*). The detailed spectroscopic characterization of TcAPXII presented in this paper contributes to the understanding of the complex structure−function relationships of peroxidases and suggests that the assignment of plant peroxidases into two classes may be too simplistic for a ubiquitous enzyme that is present in all higher plants examined to date. TcAPXII is a new paradigm peroxidase since it is the first example of a hybrid enzyme that combines spectroscopic signatures, structural elements, and substrate specificities previously only reported for distinct class I and class III peroxidases.

EXPERIMENTAL PROCEDURES

The purification of cationic ascorbate peroxidase isoenzyme II (TcAPXII) from tea leaves of *Camelia sinensis* var. *sinensis*, clone BBK35, has been reported previously (*18*). Tea leaves frozen in dry ice were supplied by Unilever Research (Colworth Bedford, U.K.). The purified protein had an Rz (A_{402}/A_{275}) value of 2.86.

TcAPXII were prepared in 25 mM malonate, titrated with NaOH to pH 5.5, or in 100 mM Tris/HCl at pH 8, or 150 mM borate/NaOH at pH 9. Benzhydroxamic acid (Aldrich, 99%) and L-(+)-ascorbic acid (Merck, 99.7%) were added from concentrated solutions, titrated with NaOH to the required pH. The fluoride complex was obtained by adding 0.1 M NaF (Merck) to the ferric protein dissolved in malonate (pH 5.5) or citrate (pH 5.0). The ferrous enzyme was obtained by adding a small volume (2−4 μL) of fresh sodium dithionite solution (10 g/L $Na_2S_2O_4 \cdot 2H_2O$) to a deoxygenated protein solution (30−40 μL). Deuterated ferrous TcAPXII was prepared by lyophilizing a sample at pH 5.5. The lyophilized material was redissolved in D_2O, and the pD was adjusted to 6.0 with DCl (*20*). The protein was then reduced by sodium dithionite in D_2O, buffered with 25 mM malonate/NaOD at the same pD, as described above. CO complexes of TcAPXII were prepared by flushing the proteins with CO (Rivoira, Italy) followed by reduction with sodium dithionite. The pH was measured directly in the sample with a microelectrode after data collection. Sample concentrations for RR experiments ranged from 26 to 90 μM for excitation at the Soret band and from 0.27 to 0.32 mM for excitation with visible light. Electronic absorption spectra were measured in solutions containing between 10 and 83 μM protein. The cyanide complex was prepared by adding 12 μL of a 100 μM TcAPXII solution in 1 mM malonate, pH 5.5, to 24 μL of a concentrated KCN (~1 M) solution in 0.5 M glycine/NaOH, pH 10.5. The TcAPXII−CN complex is unstable at acid pH; thus spectra could only be recorded at alkaline pH. Prior to exposure to the laser beam, the electronic absorption spectrum at pH 6 contains a weak band at 670 nm. This band increases upon exposure to the laser beam, which is indicative of verdoheme formation (*21*).

Resonance Raman spectra were obtained by excitation with the 406.7, 413.1, and 568.2 nm lines of a Kr^+ laser (Coherent, Innova 90/K), the 514.5 nm line of an Ar^+ laser (Coherent, Innova 90/5), and a 441.6 nm Hg/Cd laser (Liconix). The backscattered light from a slowly rotating NMR tube was collected and focused into a computer-controlled double monochromator (Jobin-Yvon HG 2S) equipped with a cooled photomultiplier (RCA C31034 A) and photon-counting electronics. The RR spectra were calibrated to an accuracy of ± 1 cm^{-1} for intense isolated bands, with indene as standard for the high-frequency region and with both indene and CCl_4 for the low-frequency region. To minimize local heating of the protein by the laser beam, the sample was cooled to approximately 15 °C by a gentle flow of N_2 gas passed through liquid N_2. Cooling was not necessary for the CO complexes because of the low laser power at the sample. In fact, the CO adducts were extremely sensitive to photolysis in the laser beam. Therefore, only very low laser power (0.7−2 mW depending on pH and protein concentration) could be applied.

Polarized spectra were obtained by inserting a polaroid analyzer between the sample and the entrance slit of the monochromator. The depolarization ratios, $\rho = I_\perp/I_{||}$, of the bands at 314 and 460 cm^{-1} of CCl_4 were measured to check the reliability of the polarization measurements. The values obtained, 0.73 and 0.00, respectively, compare well with the theoretical values of 0.75 and 0.00. To determine peak intensities and positions, a curve-fitting program was used to simulate experimental spectra, using Lorentzian line

shapes. The frequencies of the bands were optimized with an accuracy of 1 cm^{-1}, and the bandwidths with an accuracy of 0.5 cm^{-1}. The following bandwidths (in reciprocal centimeters) were used in the simulations of the high-frequency spectra of the ferric state: ν_3, 13.5; ν_{38}, ν_{11}, ν_2, and ν_{37}, 18.5; ν_{19}, 16.0; ν_{10}, 10.5; ν(C═C), 11.5; and for overlapping $\nu_{10} + \nu$(C═C) at 1620 cm^{-1}, 11.0. To simulate the low-frequency spectra of the ferrous state, the bandwidths were 12.0 cm^{-1} for porphyrin modes $\leq$293 cm^{-1}, 15.0 cm^{-1} for the bands at 311 and 323 cm^{-1}, and 16.0 cm^{-1} for ν-(Fe−Im).

Electronic absorption spectra were recorded at room temperature (23 ± 1 °C) with a double-beam Cary 5 spectrophotometer. Electronic absorption spectra were recorded both prior to and after RR measurements to check if degradation had occurred under the experimental conditions. No changes were observed in the electronic absorption spectra between pH 7 and 5.5 prior to laser illumination. However, during the RR measurements of the ferric form at pH 7, the sample became fluorescent and both a 6cLS heme species and verdoheme, characterized by a band around 670 nm in the electronic absorption spectrum, were formed in the laser beam. On the contrary, at pH 5.5 no changes were observed even after prolonged exposure. It has been reported that both the stability and activity of TcAPXII are highest at acidic pH and that addition of excess H_2O_2 at pH 7 results in verdoheme rather than compound III (*18*). Prior to laser illumination, a small amount of LS heme was observed in the UV−vis spectrum of the ferric protein above pH 9. Therefore, the spectroscopic characterization of ferric TcAPXII was performed at pH 5.5.

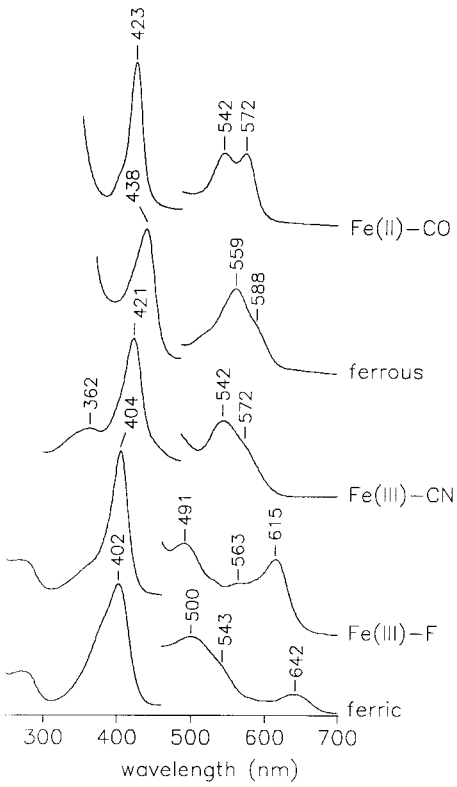

FIGURE 1: Electronic absorption spectra of TcAPXII. The samples are in 25 mM malonate/NaOH, pH 5.5, except for the cyanide complex, which is in 0.33 M glycine/NaOH, pH 10.5. The fluoride complex is obtained with 0.1 M NaF and the ferric cyanide complex with ~0.7 M KCN. The ferrous state is made by adding 1 g/L sodium dithionite, and the CO complex is made by flushing the ferrous protein with CO. The visible ranges are 5-fold expanded (fluoride complex, 10-fold).

RESULTS AND DISCUSSION

Substrate Binding. Many plant and fungal peroxidases bind the aromatic substrate analogue benzhydroxamic acid (BHA) to yield a 6c aquo species, characterized by an intense, narrow, and red-shifted Soret band compared to the 5c form (*22*). Spectrophotometric titration data yield dissociation constants (K_d) varying from 2.6 μM for the BHA complexes of HRPC to 3.7 mM for ARP/CIP (*22*−*24*). No changes are observed in the TcAPXII spectrum upon addition of 10 mM BHA. At higher concentrations, the difference between the spectra with and without BHA reveals a band at 407 nm with an intensity that increases with BHA concentration (data not shown). In the presence of 143 mM BHA, the intensity of this band is 15% of the total Soret band, which is 1 nm red-shifted. This effect is pH-independent, with similar changes observed at pH 5.5, 7.3, and 9.0, apart from a small amount of a LS species at pH 9, as deduced from the weak shoulder around 420 nm. The lack of BHA effects on the Soret band allows an estimate of $K_d > 150$ mM. Although BHA does not induce a shift in the Soret band, the compound does effectively inhibit the oxidation of guiacol with a I_{50} between 0.1 and 0.3 mM (data not shown).

Although TcAPXII has a very high specific activity for ascorbate at pH 4.5 (*18*), no changes in the electronic absorption spectrum were observed upon addition of up to 200 mM ascorbate to the ferric state at both pH 4.5 and 5.5. Only at very high concentrations of ascorbate at pH 4.5 (>0.2 M) was a slight increase of 6c species observed. This is most likely to be due to nonspecific binding, ionic strength, or the high viscosity of the solution (data not shown). In plant cells, up to 50 mM ascorbate is present in the chloroplasts (*25*). Hence, the presence of ascorbate at physiologically relevant concentrations does not alter the coordination or spin state of the heme in TcAPXII.

Ferric State and Ligand Binding. Figure 1 compares the electronic absorption spectra of ferric TcAPXII and its fluoride and cyanide complexes. The spectrum of the ferric form, very similar to that of ferric HRPC, is characterized by a Soret band at 402 nm, Q-bands at 500 and 543 nm, and a CT1 band at 642 nm, suggesting the presence of a mixture of spin species. Upon addition of KCN to TcAPXII the spectrum becomes typical of a CN-bound 6cLS heme complex, with a Soret band at 421 nm and Q-bands at 542 and 572 nm. In the presence of NaF, the Soret band of ferric TcAPXII sharpens and upshifts by 2 nm to 404 nm with a concomitant blue shift of the CT1 band to 615 nm. The Soret band at 404 nm is identical to that of the HRPC fluoride complex, whereas the charge-transfer band is 4 nm red-shifted relative to that of HRPC (*26*). However, the spectrum of the TcAPXII−F complex is very similar to that of the APX−F complex, which shows a Soret band at 403 nm and a CT1 band at 616 nm (*27*). Since the TcAPXII−F spectra are identical both in 25 mM malonate, pH 5.5, and in 50 mM citrate, pH 5.0 (data not shown), an artifact induced by use of a different buffer, pH, or ionic strength is extremely unlikely.

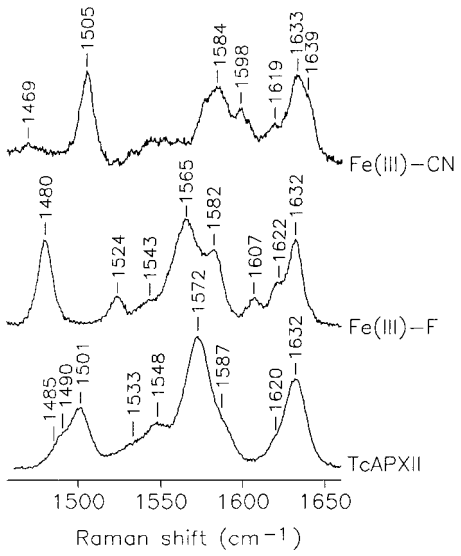

FIGURE 2: Resonance Raman spectra (high-frequency region) of TcAPXII, the fluoride complex at pH 5.5 (25 mM malonate/NaOH), and the cyanide complex at pH 10.5 (0.33 M glycine/NaOH, pH 10.5). Experimental conditions: 5 cm^{-1} spectral resolution; (TcAPXII and fluoride complex) 406.7 nm excitation wavelength, 10 mW laser power, 45 s/0.5 cm^{-1} (TcAPXII) and 10 s/0.5 cm^{-1} (fluoride) collection interval; (cyanide complex) 413.1 nm excitation wavelength, 15 mW laser power, 15 s/0.5 cm^{-1} collection interval.

The electronic absorption spectrum of the fluoride complex is a sensitive indicator of hydrogen-bonding interactions between the bound ligand and distal amino acid residues (*26, 27*). In peroxidases the distal Arg and His residues are extremely important in stabilizing bound anionic ligands. Furthermore, in class I peroxidases that contain a distal Trp residue, fluoride is stabilized by an additional hydrogen bond with this residue. This extra H-bond causes a red shift of the CT1 band by 4−5 nm with respect to the peroxidases of class II and III (*26, 27*). Thus when fluoride acts as a hydrogen-bond acceptor, the increase in the number and strength of the hydrogen bonds is manifested by the longer wavelength of the CT1 band (*26*). Therefore, the red shift of the CT1 band in the TcAPXII−F complex is due to the presence of an additional strong hydrogen bond between the fluoride ligand and a distal residue in TcAPXII that is not present in HRPC.

The high-frequency region RR spectra of the ferric TcAPXII and its fluoride and CN complexes obtained with Soret excitation are shown in Figure 2. Inspection of the ν_3 region gives the clearest indication of the population of the heme spin forms, since the ν_3 mode is in a spectral region free from overlap with other bands. For the ferric protein the ν_3 region shows three bands at ∼1485, 1490, and 1501 cm^{-1}, the latter band being dominant. This frequency can be interpreted as either a 6-coordinate (6c) low-spin (LS) heme or a 5-coordinate (5c) quantum mechanically mixed-spin heme (QS) species, the latter resulting from the admixture of high-spin ($S = {}^5/_2$) and intermediate-spin ($S = {}^3/_2$) heme spin states. A 5cQS heme is characterized by an overall blue shift of the electronic absorption spectrum compared to typical HS hemes, a CT1 band around 630−635 nm, and high RR core size marker band frequencies close to those of a LS heme (*28*−*32*). An increase of the contribution from the $S = {}^3/_2$ state in the quantum mechanically mixed-spin heme causes an increase of the frequencies of the core size marker bands. Since no LS heme is detected in the electronic absorption spectrum, the band at 1501 cm^{-1} is assigned to the ν_3 mode of a 5cQS species and the two shoulders at 1490 and 1485 cm^{-1} are assigned to the ν_3 modes of a 5cHS and a 6cHS species, respectively.

To confirm the assignment we used different excitation wavelengths and polarized light. With Soret excitation, polarized (p) bands due to the totally symmetric porphyrin modes (A_{1g}) and the ν(C═C) vinyl stretching modes are enhanced via the A-term. The depolarized (dp) bands due to the non-totally symmetric modes (B_{1g}) are also observed in the Soret excitation by enhancement via the Jahn−Teller mechanism. In addition, the B_{1g} modes and the inversely polarized (ip) bands (A_{2g}) are enhanced via the B-term in Q-band excitation (*33, 34*). Figure 3A compares the high-frequency region RR spectra of the ferric form of TcAPXII at pH 5.5 taken with Soret (406.7 nm) and visible (514.5 and 568.2 nm) excitation and in polarized light. The spectrum taken with Soret excitation shows that the three bands in the ν_3 region are polarized. The ν_2 region shows an asymmetric polarized band centered at 1572 cm^{-1} with a shoulder at 1587 cm^{-1} (ν_{37}). At higher frequency two bands at 1620 and 1632 cm^{-1} are observed. In the spectrum taken with 514.5 nm excitation, the band at 1572 cm^{-1} in the nonpolarized spectrum is centered at 1570 cm^{-1} with parallel polarized light and at 1573 cm^{-1} with perpendicular polarization. Deconvolution of the spectra by curve fitting shows that this band can be resolved into two inversely polarized bands at 1569 and 1575 cm^{-1} (data not shown). They are assigned to two ν_{19} modes of 5cHS and 5cQS, respectively. The other bands, observed in the 1520−1600 cm^{-1} region, are assigned to ν_{11} (1548 cm^{-1}, dp), ν_2 (1572 cm^{-1}, p), and ν_{37} modes (1587 cm^{-1}, p), respectively.

In the 1600−1650 cm^{-1} region of the RR spectra, bands due to the ν(C═C) and ν_{10} modes overlap with all three excitations, as previously observed for other peroxidases, namely, CCP (*35*), HRPC (*36*), and CIP (*37*). Deconvolution of these spectra by curve fitting (Figure 3B) shows a polarized band at 1632 cm^1, assigned to a ν(C═C) mode, and two depolarized bands at 1637 and 1628 cm^{-1}, which are assigned to ν_{10} modes of 5cQS and 5cHS species, respectively. A fourth band at 1620 cm^{-1} has an apparent polarization ratio of 0.5 with both 406.7 and 514.5 nm excitation. We suggest that it is due to the second ν(C═C) mode, overlapping with the ν_{10} of a 6cHS species. No 6cLS heme was observed in the RR spectra obtained with excitation at 568.2 nm, i.e., in resonance with the Q-band of the 6cLS form.

The assignment of the most intense RR bands of ferric TcAPXII and its complexes with fluoride and cyanide is shown in Table 1. Ferric TcAPXII at pH 5.5 is mainly characterized by a 5cQS species, coexisting with 5c- and 6cHS species. The electronic absorption and RR spectra of TcAPXII very closely resemble those of HRPA2 (29) and SBP (*27*). These peroxidases belong to class III and contain a 5cQS heme, coexisting with 5c- and 6cHS hemes. In HRPC, the main species were assigned to a 5cQS and a 6cQS species (*29, 36, 38, 39*). Compared to the RR spectrum of HRPC, the frequencies of the ν_3, ν_{19}, and ν_{10} modes of the QS species of TcAPXII are 1−2 cm^{-1} higher, suggesting that the QS species of TcAPXII has an increased contribution of the intermediate spin state compared to HRPC. This is in

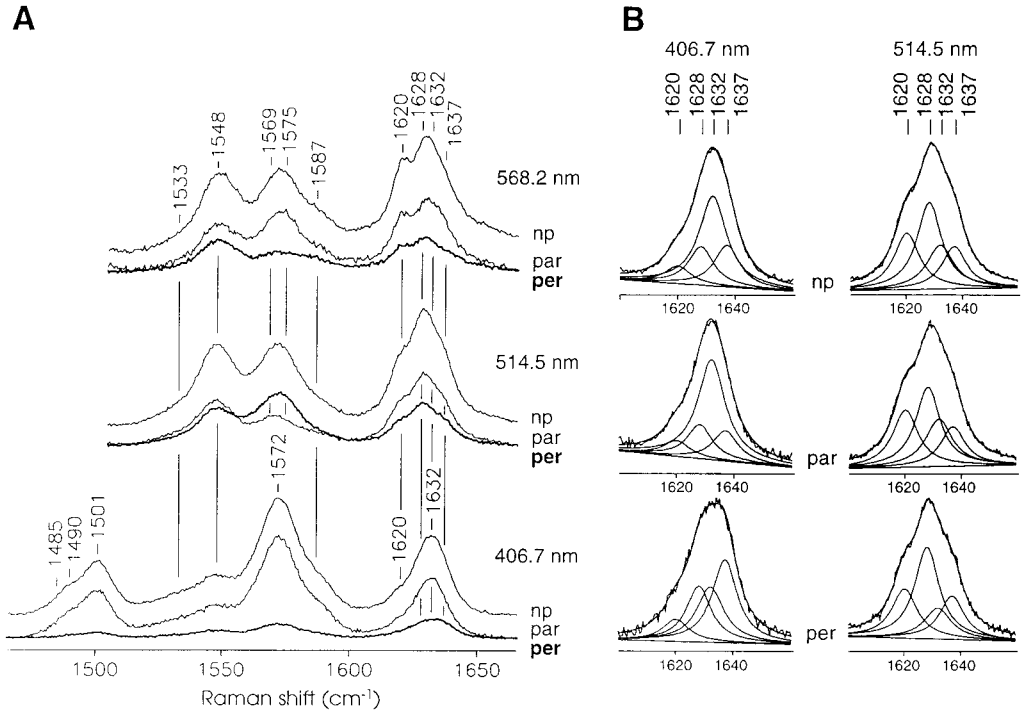

FIGURE 3: (A) Resonance Raman spectra (high-frequency region) of TcAPXII at pH 5.5 (25 mM malonate/NaOH) taken with excitation at 406.7, 514.5, and 568.2 nm and in polarized light. Experimental conditions: 5 cm^{-1} spectral resolution; (406.7 nm) 10 mW laser power at the sample, 45 s/0.5 cm^{-1} (nonpolarized, np), 16 s/0.5 cm^{-1} (parallel, par), and 32 s/0.5 $cm-1$ (perpendicular, per) collection interval; (514.5 nm) 60 mW laser power at the sample, 28 s/0.5 cm^{-1} (np), 20 s/0.5 cm^{-1} (par), and 15 s/0.5 cm^{-1} (per) collection interval; (568.2 nm) 100 mW laser power at the sample, 56 s/0.5 cm^{-1} (np), 30 s/0.5 cm^{-1} (par), and 30 s/0.5 cm^{-1} (per) collection interval. (B) Deconvolution of the ν_{10}/ν(C═C) regions with 406.7 and 514.5 nm excitation wavelengths. The frequencies of the fitted bands are 1620, 1628, 1632, and 1637 cm^{-1}. Band assignments and depolarization ratios are listed in Table 1.

Table 1: Resonance Raman Frequencies for Heme Spin State of Ferric TcAPXII and Its Adducts with Cyanide and Fluoride[a]

mode	sym	pol	5cQS	5cHS	6cHS	6cHS (F)	6cLS (CN)
ν_3	A_{1g}	p	1501 (0.12)	1490 (0.12)	1485 (0.12)	1480	1505
ν_{38}	E_u	p	1533 (0.22)[b]			1524	
ν_{11}	B_{1g}	dp	1548 (0.79)[b]			1543	
ν_2	A_{1g}	p	1572 (0.14)[b]			1565	1584
ν_{19}	A_{2g}	ip	1575 (2.74)	1569 (1.74)			
ν_{37}	E_u	p	1587 (0.47)[b]			1582	1598
ν_{10}	B_{1g}	dp	1637 (0.66)	1628 (0.68)	1620 (0.48)[c]	1607	1639
ν(C═C)		p	1620 (0.48)[b,c]			1622	1619
ν(C═C)		p	1632 (0.18)[b]			1632	1633

[a] Resonance Raman frequencies are given in reciprocal centimeters. Depolarization ratio is given in parentheses. Sym, symmetry; pol: polarization; 5cQS, 5-coordinate quantum mechanically mixed-spin; 5cHS, 5-coordinate high-spin; 6cHS, 6-coordinate high-spin; 6cLS, 6-coordinate low-spin. [b] The band is in common for all species. [c] Overlapping ν_{10} and ν(C═C) bands.

agreement with the 1 nm blue shift of the electronic absorption spectrum of TcAPXII.

The high-frequency of the RR spectra of the TcAPXII−F and TcAPXII−CN complexes taken with excitation at 406.7 nm are characteristic of 6cHS and 6cLS hemes, respectively (Figure 2 and Table 1). Since for both complexes, the ν_{10} band (at 1607 and 1639 cm^{-1}, respectively) does not overlap the vinyl bands, the ν(C═C) stretches of the vinyl substituents can be easily identified at 1622 and 1632 cm^{-1} for the fluoride complex and at 1619 and 1633 cm^{-1} for the cyanide complex. These frequencies are very similar to those observed for the ferric protein (Table 1). On the basis of RR spectra and local density functional calculations on mono- and divinylhemins, it has been proposed that when the protein matrix exerts no constraints on the vinyl groups, two distinct ν(C═C) stretching modes should be observed in their RR spectrum. The calculations suggest that one band, around 1620 cm^{-1}, can be assigned to a nearly in-plane vinyl group pointing toward the β-pyrrole methyl group, and the other band, around 1630 cm^{-1}, to an out-of-plane vinyl group pointing toward the *meso*-hydrogen of the heme (*40*). X-ray structures of peroxidases show that the dihedral angle of vinyl 2 varies widely, whereas the angles of vinyl 4 vary over a smaller range. Accordingly, the RR ν(C═C) stretching frequencies vary from about 1618 to 1632 cm^{-1} (*26*). The higher the frequency of the vinyl stretch, the less conjugated is its double bond with the porphyrin macrocycle (*31*). The X-ray structure of recombinant CCP (*41*) shows that both vinyls are oriented parallel to the pyrrole double bond due to the steric hindrance of the bulky Met172 residue in close proximity to vinyl 2, and both RR ν(C═C) are found to overlap at 1620 cm^{-1} (*42*). Met172 has been replaced by a less bulky Ser residue in class III peroxidases and pea APX. Consequently, vinyl 2 is less constrained and two vinyl stretching bands (at about 1620 and 1630 cm^{-1}) are observed in the RR spectra of these proteins (*27*, *31*). The RR spectra of ferric TcAPXII and of its complexes clearly show two ν(C═C) bands, suggesting that vinyl 2 has an out-of-plane orientation due to the presence of a serine, or a similarly sized, residue.

The low-frequency region of the RR spectrum of ferric TcAPXII and its fluoride and cyanide adducts taken with Soret excitation are shown in Figure 4. Several bands of ferric

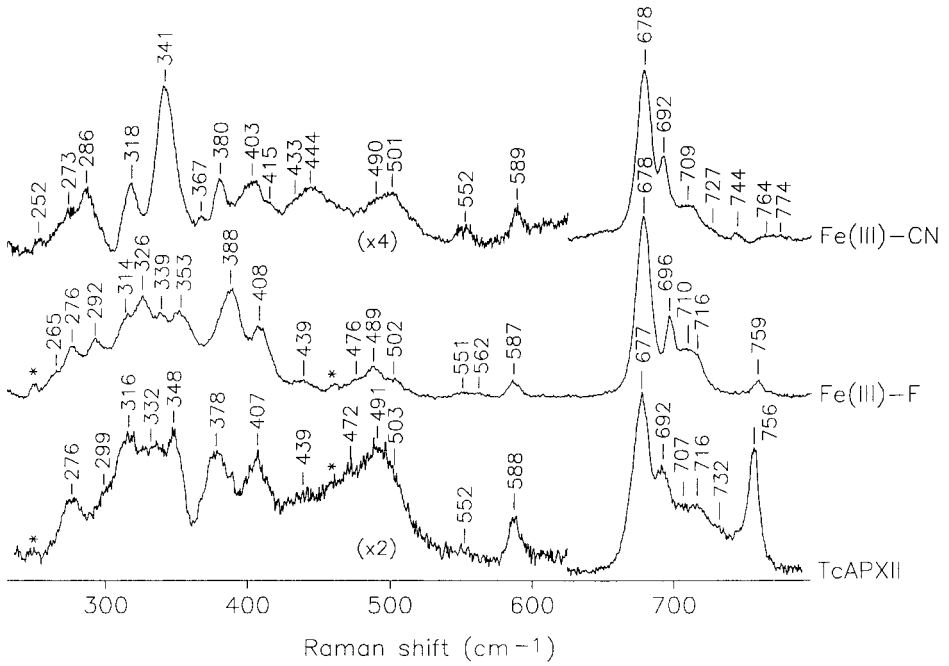

FIGURE 4: Resonance Raman spectra (low-frequency region) of TcAPXII, the fluoride complex at pH 5.5 (25 mM malonate/NaOH), and the ferric cyanide complex at pH 10.5 (0.33 M glycine/NaOH, pH 10.5). The spectra of ferric TcAPXII and the cyanide complex are 2-fold and 4-fold expanded, respectively, for frequencies <625 cm^{-1}. Experimental conditions: 5 cm^{-1} spectral resolution, 15 mW laser power at the sample; (TcAPXII) 406.7 nm excitation wavelength, 30 s/0.5 cm^{-1} collection interval for frequencies <365 cm^{-1} and 15 s/0.5 cm^{-1} collection interval for frequencies >365 cm^{-1}; (fluoride complex) 406.7 nm excitation wavelength, 10 s/0.5 cm^{-1} collection interval; (cyanide complex) 413.1 nm excitation wavelength, 39 s/0.5 cm^{-1} collection interval in the frequency range 295−545 cm^{-1}, and 19 s/0.5 cm^{-1} collection interval for frequencies <295 cm^{-1} and >545 cm^{-1}. The asterisks indicate laser plasma lines.

TcAPXII as well as of its fluoride complex have a low intensity compared to HRPC (*43*); therefore they cannot be unambiguously assigned. The spectra of both the free protein and fluoride adduct are very complex as previously observed for other peroxidases belonging to class III, namely, HRPC, HRPA2, and SBP (unpublished data). Therefore, a full assignment of the bands is not straightforward without reconstitution of the protein with isotopically labeled hemes. However, on the basis of the comparison of the spectra obtained for the CN complex, a tentative assignment of several bands can be made. The RR spectrum in the low-frequency region of the cyanide adduct can assist in the assignment of the out-of-plane modes in the RR spectra of both the ferric and Fe−F complex. Upon CN binding the heme becomes typical of a 6cLS heme and some of the out-of-plane modes, expected to be active in the high-spin complexes, are lost in the low-spin adducts (*44*). Since the spectrum of the TcAPXII−CN adduct closely resembles that of metmyoglobin−CN (metMb−CN) (*44*), the bands at 318, 341, 380, and 403 cm^{-1} are assigned accordingly to the γ_{16}, ν_8, $\delta(C_\beta C_c C_d)$ bending mode of the propionate groups, and $\delta(C_\beta C_a C_b)$ bending mode of at least one vinyl group, respectively. The bands at similar frequencies in the spectra of the ferric form and the fluoride adduct are assigned in the same way. The band at 332 cm^{-1} in the ferric protein (at 326 cm^{-1} in the fluoride adduct), which disappears in the CN complex, is tentatively assigned to the out-of-plane mode γ_6 on the basis of frequency similarities with nickel octaethylporphyrin (NiOEP) (*45*), metMb (*44*), and CCP (*42*). A much lower intensity is observed for the band around 710 cm^{-1} (716 cm^{-1} for HRPC). However, this band is broad in the TcAPXII spectra and split in two bands for the fluoride complex at low temperature (data not shown). The high intensities of the corresponding bands in the HRPC spectra might, therefore, be due to an overlap of different modes. The frequencies are similar to those of the out-of-plane modes γ_5, γ_{11}, and γ_{15} found for NiOEP (*45*) and metMb (*44*). A lower intensity (compared to HRPC) is observed also for the bands of the ferric TcAPXII at 378 cm^{-1}, assigned to the bending mode of the propionate groups of the heme, by analogy with the corresponding band observed in metMb (*44*). The corresponding mode in the fluoride adduct is assigned to the band at 388 cm^{-1}. This band in the TcAPXII spectrum has a lower intensity compared to that in the HRPC spectrum. However, this difference was also observed in the spectra of the ferric state without fluoride. The ν(Fe−F) stretching mode is also expected to be in this region of the RR spectrum. Its frequency would provide direct evidence for hydrogen bonding of the fluoride ligand to distal residues in TcAPXII. For HRPC, the ν(Fe−F) is observed at 385 cm^{-1} upon excitation in the CT1 band (*46*). The fact that this frequency is lower than that of the globins by 70−80 cm^{-1} (*47*) is in agreement with the presence of stronger hydrogen bonding between the fluoride and distal residues. However, the ν(Fe−F) band could not be identified in the spectra of the fluoride complexes of HRPC, CCP, and CIP from the Soret excitation (from 406.7 to 457.9 nm), which is available to us. Therefore, the ν(Fe−F) stretch is very weak in peroxidases and possibly overlaps with the propionate bending modes (*48*). The same conclusion is drawn here for the TcAPXII−F complex: the bands observed in the 370−390 cm^{-1} region for TcAPXII are assigned to the propionate bending modes. They are at higher frequencies and have lower intensities compared to those of HRPC. The higher frequency of the propionate bands is indicative of either a strengthening or an increase in the number of their hydrogen

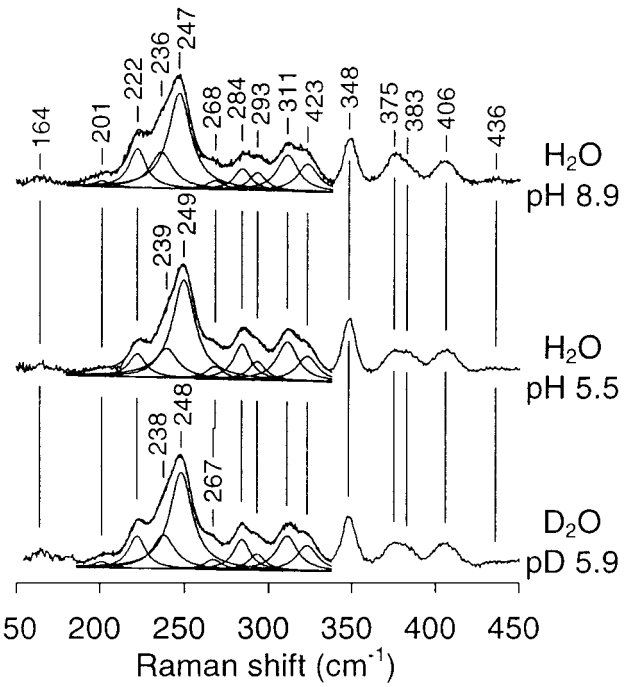

FIGURE 5: Resonance Raman spectra (low-frequency region) of ferrous TcAPXII at pH 8.9 (100 mM borate/NaOH), pH 5.5 (25 mM malonate/NaOH), and in D_2O at pD 5.9 (25 mM malonate/NaOD). Experimental conditions: 5 cm^{-1} spectral resolution, 441.6 nm excitation wavelength, 25 mW laser power at the sample; (pH 8.9) 23 s/0.5 cm^{-1} collection interval; (pH 5.5) 33 s/0.5 cm^{-1} collection interval; (pD 5.9) 25 mW laser power at the sample, 44 s/0.5 cm^{-1} collection interval for frequencies <305 cm^{-1} and 21 s/0.5 cm^{-1} collection interval for frequencies >305 cm^{-1}. The 185−335 cm^{-1} regions of the spectra were deconvoluted by curve-fitting to nine bands with Lorentzian line shapes.

bonds (*49*, *50*). Therefore, the hydrogen-bond interactions between the propionates and the protein matrix are stronger and/or more numerous in TcAPXII than in HRPC.

Ferrous State and Ligand Binding. The electronic absorption spectrum of ferrous TcAPXII at pH 5.5 (Figure 1) is very similar to that of ferrous HRPC at pH 7 and is typical of a 5cHS ferrous heme. The spectrum does not change up to pH 9, but at higher pH a 6cLS species is observed with a $pK_a = 10.8$, as determined by pH titration (data not shown). The high-frequency regions of the RR spectra with 441.6 nm excitation at both pH 5.5 and 8.9 are also typical of a 5cHS ferrous heme and similar to that of ferrous HRPC (data not shown). The vinyl stretching modes are found at 1619 and 1628 cm^{-1}, as compared to 1620 and 1627 cm^{-1} for HRPC (*37*).

Figure 5 compares the RR low-frequency region of ferrous TcAPXII at pH 5.5 and 8.9 and pD 5.9. As in HRPC, the relative intensities of the bands at 375 and 383 cm^{-1}, assigned to the propionate bending modes, change on increasing the pH (unpublished data). Similar to the ferric TcAPXII form, the intensity of the band at 348 cm^{-1}, assigned to the ν_8 mode, is lower than the corresponding band of HRPC. In the region 200−250 cm^{-1}, ferrous heme proteins are characterized by the presence of a strong band due to the ν(Fe−Im) stretching mode. A common characteristic of peroxidases is the polar hydrogen bond between the N_δ atom of the imidazole fifth ligand and the carboxylate group of an Asp residue, which gives the proximal histidine imidazolate character and results in both a strengthening of the Fe−His bond and a higher frequency as compared to other heme proteins. TcAPXII shows a broad asymmetric band at 249 cm^{-1} instead of the sharp band at 244 cm^{-1} observed for HRPC (*43*). Deconvolution of the spectrum at pH 5.5 in the region 180−340 cm^{-1} yields a shoulder at 239 cm^{-1}, with an intensity that is about $^1/_3$ that of the main band at 249 cm^{-1}. Experiments either in D_2O or at alkaline pH affect the frequencies of both bands but not their relative intensities. In particular, in D_2O the overall band downshifts by 1 cm^{-1}, and at pH 8.9, the band at 249 cm^{-1} downshifts by 2 cm^{-1} and the shoulder by 3 cm^{-1}. Therefore, on the basis of the frequency shift observed at alkaline pH and in deuterated buffer, the bands at 249 and 233 cm^{-1} are assigned to two ν(Fe−Im) stretching modes. The absence of a decrease of the I_{249}/I_{239} intensity ratio between the two bands at alkaline pH suggests that the two species are independent and not in equilibrium, as previously found for ferrous APX (*27*).

The CO complex of ferrous TcAPXII is readily formed and stable when kept under a CO atmosphere. The electronic absorption spectrum of the CO complexes of TcAPXII is identical to that of HRPC−CO with bands at 423, 542, and 572 nm (Figure 1). Figure 6A shows the low-frequency RR spectra of the TcAPXII−CO complex obtained at various pH values in the presence of ^{13}CO and ^{12}CO. A broad asymmetric band, centered at 537 cm^{-1} with a shoulder at about 545 cm^{-1}, is observed for the ^{12}CO complex at pH 5.0. These bands shift down by 6 and 5 cm^{-1}, respectively, in the ^{13}CO complex. Therefore, they are assigned to two ν(Fe−CO) stretching modes corresponding to the acid form. At pH 5.5 the RR spectrum is characterized by the appearance of a new band at 516 cm^{-1} with the concomitant decrease of the broad band at 537 cm^{-1}. At pH 7.9, the band at 516 cm^{-1} becomes dominant and a shoulder at about 503 cm^{-1} is observed. The band at 516 cm^{-1} displays an isotopic shift of 6 cm^{-1} while the shoulder shifts down by about 5 cm^{-1}.These two bands are assigned to two other ν(Fe−CO) stretching modes. In the TcAPXII−^{13}CO complex at pH 7.9 there is an additional isotope-sensitive band. The shoulder at approximately 580 cm^{-1}, which overlaps with the porphyrin mode at 588 cm^{-1}, shifts to 564 cm^{-1}. The position and the relatively large isotopic shift of this band allows its assignment to the δ(FeCO) bending mode. At acid pH the corresponding mode is not observed. At pH higher than 9 or lower than 4.5, the protein is not stable and denatures or partially unfolds (data not shown).

The corresponding FT-IR spectra of the TcAPXII Fe(II)−CO complexes are shown in Figure 6B. At pH 5.0, two strong bands at 1892 and 1908 cm^{-1} and two weak bands at 1930 and 1946 cm^{-1} are observed. They shift to 1848, 1866, 1883, and 1900 cm^{-1}, respectively, when ^{12}CO is replaced by ^{13}CO. Therefore, they are assigned to four ν(CO) stretches. At alkaline pH the relative intensity of the bands changes: the bands at 1930 and 1946 cm^{-1} become dominant with the concomitant disappearance of the other two bands. At pH 5.5 the four bands are all present with intermediate intensity, in agreement with the RR spectrum. On the basis of the relative intensities and frequencies of the bands, four different conformers of the TcAPXII Fe(II)−CO complex are evident both in the IR and in the RR spectra. The RR ν(FeC) bands at 537 and 545 cm^{-1}, dominant at acid pH, correspond to the IR ν(CO) bands at 1892 and 1908 cm^{-1}, respectively, whereas the dominant ν(FeC) bands observed

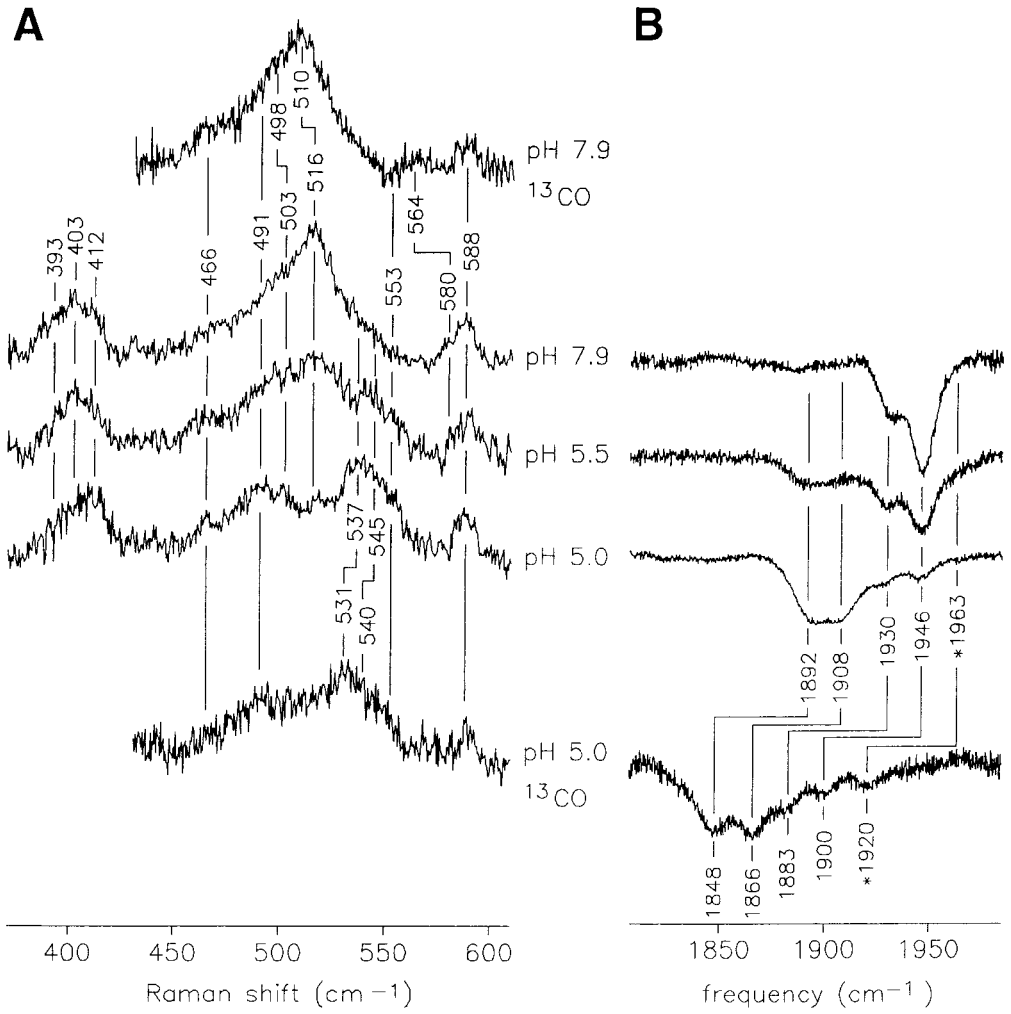

FIGURE 6: CO complexes of ferrous TcAPXII at pH 5.0 (0.2 M citrate/NaOH), pH 5.5 (25 mM malonate/NaOH or 50 mM MES/NaOH), and pH 7.9 (0.1 M Tris/HCl). (A) Resonance Raman spectra (low-frequency region). Experimental conditions: 7 cm^{-1} spectral resolution (5 cm^{-1} at pH 5.5), 413.1 nm excitation wavelength; (^{13}CO, pH 7.9) 1.9 mW laser power at the sample, 59 s/0.5 cm^{-1} collection interval; (^{12}CO, pH 7.9) 1.6 mW laser power at the sample, 141 s/0.5 cm^{1} collection interval; (^{12}CO, pH 5.5) 1.1 mW laser power at the sample, 201 s/0.5 cm^{-1} collection interval; (^{12}CO, pH 5.0) 0.9 mW laser power at the sample, 182 s/0.5 cm^{-1} collection interval; (^{13}CO, pH 5.0) 0.7 mW laser power at the sample, 75 s/0.5 cm^{-1} collection interval. (B) Fourier transform infrared spectra. Experimental conditions: 0.2 cm^{-1} spectral resolution; (pH 7.9) 6500 scans accumulated; (pH 5.5) 6000 scans accumulated; (^{12}CO and ^{13}CO, pH 5.0) 8000 scans accumulated. The asterisks indicate the bands due to the CO complex of denatured enzyme.

at alkaline pH at 516 and 504 cm^{-1} correspond to the IR ν(CO) bands at 1930 and 1946 cm^{-1}, respectively. It must be stressed that neither the ν(FeC) at 545 cm^{-1} nor the ν-(CO) band at 1892 cm^{-1} has ever been observed in any other heme protein.

Carbon monoxide is a sensitive probe for investigating proximal ligand and distal environmental effects. In particular, steric hindrance on the bound CO exerted by distal residues, their polarity, and formation of hydrogen bonds increases back-donation from the Fe d_π to the CO π* orbitals. As a consequence, the Fe−CO bonds strengthen while the C−O bonds weaken, thereby increasing the ν(Fe−C) vibrational frequencies and decreasing the ν(CO) frequencies (*51*−*53*). For a large class of CO−porphyrin adducts, including heme proteins and model compounds containing an imidazole as fifth ligand, a linear correlation between the frequencies of the ν(Fe−C) and the ν(CO) stretching modes has been found (*53*, *54*). The correlation has a negative slope and depends on the extent of π back-bonding. It has recently been proposed that, among the various factors, it is the polarity that is the key determinant. The electrostatic fields generated by polar distal pocket amino acids alter the electron distribution in the Fe−CO complex, changing the order of the CO bond and accordingly its vibrational frequencies (*52*).

Figure 7 shows a plot of ν(Fe−C) versus ν(CO) frequencies for the CO adducts of TcAPXII, compared with those observed for CCP and HRPC, as reported in Table 2. HRPC at pH 6.0 shows two conformers. In form I the oxygen atom of the bound CO mainly interacts with the positively charged guanidinium group of the distal Arg via a hydrogen bond. In the second HRPC−CO (form II) conformer, the oxygen atom of the bound CO molecule mainly interacts with the distal His via a hydrogen bond. (*55*). The CCP−CO adduct at pH 6.0 shows only one conformer characterized by vibrational frequencies corresponding to a weaker interaction with CO than in form I of HRPC. It was, therefore, assigned to CO hydrogen-bonded with the distal Arg (*56*, *57*) via a water molecule, as observed in the X-ray structure of the CO complex (*58*). In CCP, at alkaline pH the interaction between the bound CO and the distal pocket is weakened with the concomitant upshift of the ν(CO) frequency and downshift of the ν(Fe−C) frequency. Finally, in the HRPC−

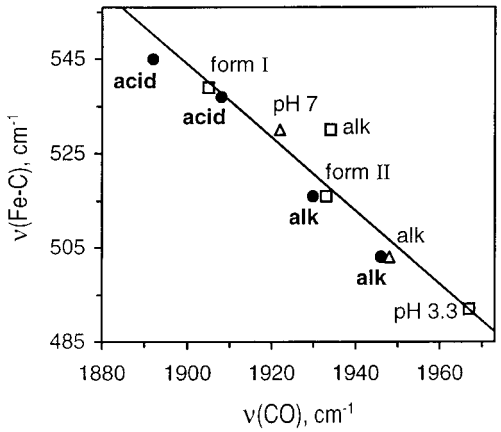

FIGURE 7: Plot of the ν(Fe−C) versus ν(CO) frequencies in the CO complexes of TcAPXII (●), HRPC (□), and CCP (△). The frequencies are listed in Table 2.

Table 2: Vibrational Frequencies of Ferrous−CO Complexes (see also Figure 7)

		ν_{CO} (cm^{-1})	$\Delta^{13}C$ (cm^{-1})	ν_{Fe-C} (cm^{-1})	$\Delta^{13}C$ (cm^{-1})	δ_{Fe-C-O} (cm^{-1})	$\Delta^{13}C$ (cm^{-1})
TcAPXII		1892	−44	545	−5	580	16
		1908	−42	537	−6		
		1930	−47	516	−6		
		1946	−46	503	−5		
HRPC[a]	form I	1905		539	−4	589	16
	form II	1933		516	−5		
	pH 3.3	1967		492	−5		
	alkaline	1934		530			
CCP[b]	pH 7	1922		530	−5	585	
	alkaline	1948		503		575	

[a] (67); (68); (69); (55); (59). [b] (56); (57).

CO adduct at pH 3.3, a conformer is observed that is characterized by very low ν(Fe−C) and very high ν(CO) frequencies, consistent with a weak or even absent interaction with the surrounding amino acids (*59*).

Upon binding of CO at pH 5.0, two conformers are found for TcAPXII. For one conformer the frequencies (537 and 1908 cm^{-1}) resemble those of HRPC form I, and therefore, we can conclude that CO is directly hydrogen-bonded to the positively charged guanidinium group of the distal Arg. The 8 cm^{-1} upshift of the ν(Fe−C) band and the 16 cm^{-1} downshift of the ν(CO) band of the second acid conformer as compared to the previous one indicate that the interaction with CO is much stronger in this form. Thus CO, like fluoride, is hydrogen-bonded in TcAPXII to a distal cavity residue that is not present in HRPC. At pH higher than 5.0, the two acid forms disappear and the spectra are dominated by two other conformers. One has vibrational frequencies (516 and 1930 cm^{-1}) very close to those of form II of HRPC−CO and is therefore assigned to CO hydrogen-bonded to the distal His. The frequencies (503 and 1946 cm^{-1}) of the last conformer suggest that, as in the alkaline CO complex of CCP, CO is not hydrogen-bonded but only experiences polar interactions. This is unlike the HRPC−CO complex at alkaline pH, which has ν(CO) and ν(FeC) frequencies (Figure 7 and Table 2) that are indicative of a hydrogen-bonded CO.

CONCLUSIONS

TcAPXII Is a 5-Coordinate Quantum Mixed-Spin Heme Peroxidase. The overall blue shift of the electronic absorption spectrum, the high RR frequencies of the core size marker bands, and the complex RR spectrum in the low-frequency region of ferric TcAPXII at pH 5.5−7.0 clearly indicate that it is characterized by a 5cQS heme. This species is very rare in nature; its origin in heme proteins remains elusive, and among the various peroxidases, it has been observed exclusively in class III peroxidases. The QS state of HRPC, HRPA2, SBP, and BP1 (*31*) differ only by the different degrees of admixture of the HS ($S = 5/2$) and IS ($S = {}^3/_2$) states that constitute the quantum mechanically mixed-spin state. The proportion of the $S = {}^3/_2$ state increases in the order HRPC < TcAPXII < HRPA2 < SBP < BP1.

The Distal Cavity of TcAPXII Has Three Residues That Hydrogen-Bond to Heme-Coordinated Exogenous Ligands. In class I peroxidases, a 4−5 nm red shift (relative to class III peroxidases) of the CT1 band of the fluoride complex is explained by three hydrogen bonds involving distal Arg, Trp, and a water molecule that is in turn hydrogen-bonded to the distal His (*26*, *27*). In class III peroxidases Trp is replaced by a Phe, leaving only Arg and His to hydrogen-bond to the fluoride. However, TcAPXII shows the red shift although Trp is replaced by a Phe (*18*). The third hydrogen bond required to explain the red shift with TcAPXII might be provided by a Thr residue (Thr37, HRPC numbering). The presence of a third hydrogen-donor residue in the distal cavity is also strongly supported by the observation of an Fe−CO conformer with an unprecedentedly high ν(Fe−C) and concomitant very low ν(CO) stretching frequencies.

TcAPXII Has a Stronger Fe−Imidazole Bond than APX. In the low-frequency RR spectrum of ferrous TcAPXII, two independent Fe−Im stretching bands have been identified (249 and 233 cm^{-1}). This result is interesting, because all class III peroxidases are characterized by a single sharp pH-dependent Fe−Im band [at 243 cm^{-1} in HRPC (*43*), at 252 cm^{-1} in HRPA2 (*43*), and at 246 cm^{-1} in SBP (*28*)]. Class I and II peroxidases are characterized by two Fe−Im stretching modes arising from tautomerism of the imidazole N_δ proton, with respect to the donor and acceptor atoms in the proximal His−Asp hydrogen bond. The component at lower frequency [i.e., at 233 cm^{-1} in CCP (*42*, *60*) and at 211 cm^{-1} in CIP (*37*)] arises from molecules in which the proton remains on the imidazole, while the component at higher frequency [i.e., at 246 cm^{-1} in CCP and at 230 cm^{-1} in CIP] arises from molecules in which the proton is transferred to the carboxylate. Two separate bands (234 and 207 cm^{-1}) arising from the Fe−Im stretch are also observed with APX (*27*). The higher ν(Fe−Im) frequencies of TcAPXII and the small downshift (1 cm^{-1}) in D_2O suggest that the proximal His ligand has partial imidazolate character in both forms. Therefore, a stronger Fe−Im bond, resulting from a stronger hydrogen bond between the N_δ atom of the imidazole fifth ligand and the oxygen atom of the aspartic acid side chain, is proposed for TcAPXII as compared to APX.

Proximal Hydrogen-Bonding Networks of TcAPXII, HRPC, and APX Are Similar. The single Fe−Im stretching band of HRPC and the two independent ν(Fe−Im) bands of pea APX, compared to the bands modulated by the His−Asp tautomeric H-bonding equilibrium of CCP, suggest a relatively rigid proximal side in HRPC and pea APX. The crystal structures of HRPC (*61*) and pea APX (*15*) show that the proximal H-bonding networks are similar and include the

Ser residue close to vinyl 2. This small residue allows an out-of-plane orientation of vinyl 2. Conversely, the crystal structure of CCP shows that the proximal H-bonding network is less extensive (*62*). Moreover, in the proximal side of the heme cavity, CCP contains a non-hydrogen-bonding residue (Phe201), whereas HRPC and pea APX have a Tyr residue (Tyr233 and Tyr190, respectively) that is H-bonded to the Asp that is in turn H-bonded to the proximal His ligand. In addition, the bulky Met residue that imposes an in-plane orientation on vinyl 2 lacks the H-bonding capability of Ser and thus further weakens the H-bonding network. The two high-frequency ν(Fe−Im) modes and observation of two ν(C═C) frequencies for TcAPXII therefore suggest that the proximal H-bonding network is similar to that of HRPC and pea APX and that subtle structural differences modulate the strength of the H-bond between Asp and His.

Imidazolate Character of the Fe−Im Bond Destabilizes Compound I. The strength of the hydrogen bond, and thus the imidazolate character of the proximal ligand, modulates not only the strength of the Fe−Im bond but also the stability of the different oxidation states of the heme. It was found that compound I of TcAPXII is rapidly converted to compound II, while HRPC forms a stable compound I. In view of the more reactive nature of compound I and the failure to detect formation of compound III under high levels of H_2O_2, it was proposed that TcAPXII has catalase−peroxidase activity that is consistent with its function in planta under oxidative stress conditions (*18*).

TcAPXII and HRPC Have Structurally Distinct Substrate Binding Sites. From the interaction between the bound CO and the distal amino acid residues, we can infer that the orientations of the distal His and Arg residues in TcAPXII are similar to those of HRPC. However, no changes are observed in the electronic absorption spectrum of TcAPXII in the presence of 10 mM BHA. HRPC exhibits pronounced changes on tight binding of BHA (K_d 2.6 μM). The X-ray structure of the HRPC− BHA complex shows that BHA penetrates the heme cavity site and forms an extensive hydrogen-bonding network with the conserved residues His42, Arg38, and Pro139 and the distal water molecule located at 2.6 Å above the heme iron (*63*).

The aromatic ring of BHA binds in a pocket formed by the distal residues His42, Phe68, Gly69, Ala140, Pro141, and Phe179. Thus hydrogen-bonded and hydrophobic interactions are necessary for the high affinity of BHA to HRPC (*13*). The absence of changes in the electronic absorption spectrum of TcAPXII with BHA and its low reactivity with phenolic substrates (*18*) must reflect structural differences between the TcAPXII and HRPC substrate binding sites. Interestingly, physiologically relevant concentrations of ascorbate [≤50 mM (*25*)] also do not change the heme RR and electronic absorption spectra of TcAPXII, despite its very high activity with ascorbate (*18*). For pea APX, it has been shown that ascorbate oxidation occurs at an alternative site in the vicinity of Cys32, Arg172, and the heme propionates. This site is well removed from the exposed δ-heme edge where aromatic substrates bind (*64*, *65*). An analogous ascorbate binding in TcAPXII is consistent with the spectroscopic and kinetic data.

TcAPXII Is a New Paradigm Peroxidase. Our detailed spectroscopic characterization of TcAPXII and comparisons with other peroxidases emphasize the complex structure−function relationships of these ubiquitous enzymes. Previous studies have shown that class I and class III peroxidases have distinct roles in vivo (*66*).

This study has shown that TcAPXII is a hybrid enzyme that combines the spectroscopic characteristics and substrate specificities of both class I and class III peroxidases.

ACKNOWLEDGMENT

Dr. Simon J. George (John Innes Centre, Norwich, U.K.) is acknowledged for recording preliminary FT-IR spectra of the TcAPXII−CO complex.

REFERENCES

1. Welinder, K. G. (1992) *Curr. Opin. Struct. Biol. 2*, 388−393.
2. Asada, K. (1992) *Physiol. Plant. 85*, 235−241.
3. Jansen, M. A. K., Malan, C., Shaaltiel, Y., and Gressel, J. (1990) *Z. Naturforsch. C45*, 463−469.
4. Jespersen, H. M., Kjærsgård, V. H., Welinder, K. G., and Østergaard, L. (1997) *Biochem. J. 326*, 305−310.
5. Karpinski, S., Reynolds, H., Karpinska, B., Wingsle, G., Creissen, G., and Mullineaux, P. M. (1999) *Science 284*, 654−657.
6. Lagrimini, L. M. (1991) *Plant Physiol. 96*, 583.
7. Bernards, M. A. and Lewis, N. G. (1998) *Photochemistry 47*, 915−933.
8. Bestwick, C. S., Brown, I. R., and Mansfield, J. W. (1998) *Plant Physiol. 118*, 1067−1078.
9. Jansen, M. A. K., Van den Noorth, R. E., Tan, A., Prinsen, E., Lagrimini, L. M., and Thorneley, R. N. F. (2001) *Plant Physiol. 126*, 1012−1023.
10. Krylov, S. N. and Dunford, H. B. (1996) *J. Phys. Chem. 100*, 913−920.
11. Normanly, J. (1997) *Physiol. Plant. 100*, 431−442.
12. Gazaryan, I. G., Lagrimini, L. M., Mellon, F. A., Naldrett, M. T., Ashby, G. A., and Thorneley, R. N. F. (1998) *Biochem. J. 333*, 223−232.
13. Veitch, N. C., and Smith, A. T. (2001) *Adv. Inorg. Chem. 51*, 107−162.
14. Smith, A. T., and Veitch, N. C. (1998) *Curr. Opin. Struct. Biol. 2*, 269−278.
15. Patterson, W. R., and Poulos, T. L. (1995) *Biochemistry 34*, 4331−4341.
16. Marquez, L. A., Quitoriano, M., Zilinskas, B. A., and Dunford, H. B. (1996) *FEBS Lett. 389*, 153−156.
17. Kvaratskhelia, M., Winkel, C., and Thorneley, R. N. F. (1997) *Plant Physiol. 114*, 1237−1245.
18. Kvaratskhelia, M., Winkel, C., Naldrett, M. T., and Thorneley, R. N. F. (1999) *J. Plant Physiol. 154*, 273−282.
19. Mittler, R., and Zilinskas, B. A. (1991) *Plant Physiol. 97*, 962−968.
20. Glasoe, P., and Long, F. A. (1960) *J. Phys. Chem. 64*, 188−190.
21. Rodriguez-Lopez, J. N., Hernandez-Ruiz, J., Garcia-Canovas, F., Thorneley, R. N. F., Acosta, M., and Arnao, M. B. (1997) *J. Biol. Chem. 272*, 5469−5476.
22. Indiani, C., Feis, A., Howes, B. D., Marzocchi, M. P., and Smulevich, G. (2000) *J. Am. Chem. Soc. 122*, 7368−7376.
23. Smith, A. T., Sanders, S. A., Thorneley, R. N. F., Burke, J. F., and Bray, R. C. (1992) *Eur. J. Biochem. 207*, 507−519.
24. Hosoya, T., Sakurada, J., Kurokawa, C., Toyoda, R., and Nakamura, S. (1989) *Biochemistry 28*, 2639−2644.
25. Dunford, H. B. (1982) *Adv. Inorg. Biochem. 4*, 41−68.
26. Neri, F., Kok, D., Miller, M. A., and Smulevich, G. (1997) *Biochemistry 36*, 8947−8953.
27. Nissum, M., Neri, F., Mandelman, D., Poulos, T. L., and Smulevich, G. (1998) *Biochemistry 37*, 8080−8087.
28. Nissum, M., Feis, A., and Smulevich, G. (1998) *Biospectroscopy 4*, 355−364.
29. Feis, A., Howes, B. D., Indiani, C., and Smulevich, G. (1998) *J. Raman Spectrosc. 29*, 933−938.

30. Howes, B. D., Schiødt, C. B., Welinder, K. G., Marzocchi, M. P., Ma, J.-G., Zhang, J., Shelnutt, J. A., and Smulevich, G. (1999) *Biophys. J. 77*, 478−492.
31. Smulevich, G. (1998) *Biospectroscopy 4*, S3−S17.
32. Indiani, C., Feis, A., Howes, B. D., Marzocchi, M. P., and Smulevich, G. (2000) *J. Inorg. Biochem. 79*, 269−274.
33. Choi, S., Spiro, T. G., Langry, K. C., Smith, K. M., Budd, D. L., and La Mar, G. N. (1982) *J. Am. Chem. Soc. 104*, 4345−4351.
34. Spiro, T. G., and Li, X.-Y. (1988) in *Biological Applications of Raman Spectroscopy* (Spiro, T. G., Ed.) pp 1−37, John Wiley & Sons, New York.
35. Smulevich, G., Wang, Y., Edwards, S. L., Poulos, T. L., English, A., and Spiro, T. G. (1990) *Biochemistry 29*, 2586−2592.
36. Smulevich, G., Paoli, M., Burke, J. F., Sanders, S. A., Thorneley, R. N. F., and Smith, A. T. (1994) *Biochemistry 33*, 7398−7407.
37. Smulevich, G., Feis, A., Focardi, C., and Welinder, K. G. (1994) *Biochemistry 33*, 15425−15432.
38. Howes, B. D., Veitch, N. C., Smith, A. T., White, C. G., and Smulevich, G. (2001) *Biochem. J. 353*, 181−191.
39. de Ropp, J. S., Mandal, P., Brauer, S. L., and La Mar, G. N. (1997) *J. Am. Chem. Soc. 119*, 4732−4739.
40. Kalsbeck, W. A., Ghosh, A., Pandey, R. K., Smith, K. M., and Bocian, D. F. (1995) *J. Am. Chem. Soc. 117*, 10959−10968.
41. Wang, J., Mauro, J. M., Edwards, S. L., Oatley, S. J., Fishel, L. A., Ashford, V. A., Xuong, N., and Kraut, J. (1990) *Biochemistry 29*, 7160−7173.
42. Smulevich, G., Hu, S., Rodgers, K. R., Goodin, D. B., Smith, K. M., and Spiro, T. G. (1996) *Biospectroscopy 2*, 365−376.
43. Teraoka, J., and Kitagawa, T. (1981) *J. Biol. Chem. 256*, 3969−3977.
44. Hu, S., Smith, K. M., and Spiro, T. G. (1996) *J. Am. Chem. Soc. 118*, 12638−12646.
45. Gersonde, K., Yu, N.-T., Lin, S. H., Smith, K. M., and Parrish, D. W. (1989) *Biochemistry 28*, 3960−3966.
46. Yu, N.-T. (1986) *Methods Enzymol. 130*, 350−409.
47. Asher, S. A., and Schuster, T. M. (1981) *Biochemistry 20*, 1866−1873.
48. Neri, F., Indiani, C., Baldi, B., Vind, J., Welinder, K. G., and Smulevich, G. (1999) *Biochemistry 38*, 7819−7827.
49. Gottfried, D. S., Peterson, E. S., Sheikh, A. G., Wang, J., and Friedman, J. M. (1996) *J. Phys. Chem. 100*, 12034−12042.
50. Cerda-Colon, J. F., Silfa, E., and Lopez-Garrica, J. (1998) *J. Am. Chem. Soc. 120*, 9312−9317.
51. Li, T., Quillin, M. L., and Olson, J. S. (1994) *Biochemistry 33*, 1433−1446.
52. Phillips, G. N. J., Teodoro, M. L., Smith, B., and Olson, J. S. (1999) *J. Phys. Chem. B 103*, 8817−8829.
53. Ray, G. B., Li, X.-Y., Ibers, J. A., Sessler, J. L., and Spiro, T. G. (1994) *J. Am. Chem. Soc. 116*, 162−176.
54. Li, X. Y., and Spiro, T. G. (1988) *J. Am. Chem. Soc. 110*, 6024−6033.
55. Feis, A., Rodriguez-Lopez, J. N., Thorneley, R. N. F., and Smulevich, G. (1998) *Biochemistry 37*, 13575−13581.
56. Smulevich, G., Evangelista-Kirkup, R., English, A., and Spiro, T. G. (1986) *Biochemistry 25*, 4426−4430.
57. Smulevich, G., Mauro, J. M., Fishel, L. A., English, A. M., Kraut, J., and Spiro, T. G. (1988) *Biochemistry 27*, 5486−5492.
58. Edwards, S. L., and Poulos, T. L. (1990) *J. Biol. Chem. 265*, 2588−2595.
59. Smulevich, G., Paoli, M., De Sanctis, G., Mantini, A. R., Ascoli, F., and Coletta, M. (1997) *Biochemistry 36*, 640−649.
60. Smulevich, G., Mauro, J. M., Fishel, L. A., English, A., Kraut, J., and Spiro, T. G. (1988) *Biochemistry 27*, 5477−5485.
61. Gajhede, M., Schuller, D. J., Henriksen, A., Smith, A. T., and Poulos, T. L. (1997) *Nat. Struct. Biol. 4*, 1032−1038.
62. Finzel, B. C., Poulos, T. L., and Kraut, J. (1984) *J. Biol. Chem. 259*, 13027−13036.
63. Henriksen, A., Schuller, D. J., Meno, K., Welinder, K. G., Smith, A. T., and Gajhede, M. (1998) *Biochemistry 37*, 8054−8060.
64. Bursley, E. H., and Poulos, T. L. (2000) *Biochemistry 39*, 7374−7379.
65. Mandelman, D., Jamal, J., and Poulos, T. L. (1998) *Biochemistry 37*, 17610−17617.
66. Dunford, H. B. (1999) *Heme Peroxidase*, John Wiley and Sons, New York.
67. Uno, T., Nishimura, Y., Tsuboi, M., Makino, R., Iizuka, T., and Ishimura, Y. (1987) *J. Biol. Chem. 262*, 4549−4556.
68. Evangelista-Kirkup, R., Smulevich, G., and Spiro, T. G. (1986) *Biochemistry 25*, 4420−4425.
69. Rodriguez-Lopez, J. N., George, S. J., and Thorneley, R. N. F. (1998) *J. Biol. Inorg. Chem. 3*, 44−52.

BI0106033